

Open Clusters as Tracers on Radial Migration of the Galactic Disk

Y.Q. Chen & G. Zhao ^{*}

¹ Key Laboratory of Optical Astronomy, National Astronomical Observatories, Chinese Academy of Sciences, Beijing, 100101, China

² School of Astronomy and Space Science, University of Chinese Academy of Sciences, Beijing 101408, China

Submitted Feb. 2020

ABSTRACT

Radial migration is an important process in the Galactic disk. A few open clusters show some evidence on this mechanism but there is no systematic study. In this work, we investigate the role of radial migration on the Galactic disk based on a large sample of 146 open clusters with homogeneous metallicity and age from Netopil et al. and kinematics calculated from *Gaia* DR2. The birth site R_b , guiding radius R_g and other orbital parameters are calculated, and the migration distance $|R_g - R_b|$ is obtained, which is a combination of metallicity, kinematics and age information. It is found that 44% open clusters have $|R_g - R_b| < 1$ kpc, for which radial migration (churning) is not significant. Among the remaining 56% open clusters with $|R_g - R_b| > 1$ kpc, young ones with $t < 1.0$ Gyr tend to migrate inward, while older clusters usually migrate outward. Different mechanisms of radial migration between young and old clusters are suggested based on their different migration rates, Galactic locations and orbital parameters. For the old group, we propose a plausible way to estimate migration rate and obtain a reasonable value of 1.5 ± 0.5 kpc/Gyr based on ten intermediate-age clusters at the outer disk, where the existence of several special clusters implies its complicate formation history.

Key words: Galaxy: disc; Galaxy: evolution; Galaxy: abundances; Galaxy: kinematics and dynamics; open clusters and associations: general

1 INTRODUCTION

Radial migration of stars in the Galactic disk is an important process as shown by observational works (Grenon 1972; Wielen et al. 1996; Haywood et al. 2008; Hayden et al. 2015) and theoretical models/simulations (Sellwood & Binney 2002; Roskar et al. 2008; Minchev et al. 2013). It has been invoked to justify many observational phenomena, such as the existence of metal-rich stars in the solar neighbourhood (Casagrande et al. 2011; Minchev et al. 2013), the substantial scatter in the age-metallicity relation (Edvardsson et al. 1993; Haywood et al. 2013), the skewness of the metallicity distributions (Hayden et al. 2015), the presence of low-velocity dispersion of $[\alpha/\text{Fe}]$ -enhanced stars in the solar neighborhood (Minchev et al. 2014).

In particular, the lack of age-metallicity relation is contrary to observations of interstellar gas and young stars in galaxies that stars born at the same epoch have very similar $[\text{Fe}/\text{H}]$ (Przybilla et al. 2008; Nieva & Przybilla 2012). A solution to the discrepancy is radial migration, first pro-

posed by Sellwood & Binney (2002). They suggested that stars and gas close to the co-rotation resonance (associated with the spiral structure) experience large changes in their positions by migrating outward and inward radially. Subsequently, more analytic and simulation works (Roskar et al. 2008; Minchev et al. 2013; Loebman et al. 2016) recognized that migration of stars (or clusters) from their birth radius of inner disk to the solar neighborhood significantly broadens local age and metallicity distributions. Besides spiral arms, minor satellites (Quillen et al. 2009) and the bar structure (Minchev & Famaey 2010) are also radial migration mechanisms. In particular, the coupling between spiral arms and bar structure (Minchev et al. 2011; Minchev et al. 2013) is found to invoke a very powerful stellar radial migration in the inner disk, while perturbations caused by minor mergers are more effective in the outer disks (Quillen et al. 2009; Bird, Kazantzidis & Weinberg 2012).

Radial migration could alter the disk structure and chemical composition of local regions via the churning process. According to Sellwood & Binney (2002), churning occurs in the presence of changing and complex non-axisymmetric patterns (over-densities) such as spiral arms, which exert torques on stars and lead to an effective change

* E-mail:cyq,gzhao@nao.cas.cn

in a star's angular momentum (or guiding radius). By conserving their angular momentum, blurring refers to orbital heating by a variety of perturbations in the in-plane or vertical direction, which may cause increasing epicycles but remain radial oscillations around the guiding radii. Usually, churning has a stronger effect than blurring on the Galactic disk because it can migrate stars by several kpc over time-scales as short as a few Gyr (Kubryk et al. 2013; Grand et al. 2016). In this work, radial migration refers to the churning process, although some works (Halle et al. 2015, 2018) include both churning and blurring in the nomenclature of radial migration.

It is important to find birth sites of stars and derive migration distances in order to investigate its effect on the Galactic disk. In this respect, Minchev et al. (2018) proposed a plausible way, for the first time, to obtain stellar birth radii based on stellar age and metallicity with the help of assumed ISM evolution profile. Recently, Feltzing et al. (2019) applied this method to the APOGEE survey and investigated the relative significance between the churning and blurring processes by using different sets of ISM profiles. It is of high interest to apply this method to open clusters in the Galactic disk. Since distances, metallicities, and particularly ages of open clusters could be more reliably estimated as compared with stars in the field, more accurate birth sites can be obtained and thus they become best tracers on the role of radial migration in the Galactic disk.

The metallicity gradient has been well established for open clusters but there is almost no age-metallicity relation (Netopil et al. 2016), which is an evidence of the role of radial migration on open clusters. In consistent with this, theoretical simulation by Martinez-Medina et al. (2018) provided strong arguments that NGC 6791 might have formed close to the inner disk of 3–5 kpc or the bulge, and strayed to the present location by radial migration. The abundance analysis by Villanova et al. (2018) also supports its origin from the bulge population. Meanwhile, it is found that NGC 6583 could have radially migrated 3.5 kpc within 1 Gyr, indicating a high migration rate of 3.5 *kpc/Gyr* (Quillen et al. 2018). In this work, we aim to perform a systematic study on a large sample of open clusters for the first time and probe the role of radial migration on the Galactic disk by estimating their migration distances and measuring the migration rates, which could provide observational constraints on theoretical mechanisms of radial migration. It is expected that reliable ages of open clusters will cast new sight not only on the evolution of the Galactic disk but also on timescale of radial migration.

2 DATA AND SAMPLE SELECTION

Although there are over 3000 open clusters in the Galaxy, only about 10% have metallicity measurements in the WEBDA database by Dias et al. (2002). These metallicities came from different sources and were derived with different methods, leading to significant uncertainties and offsets. Netopil et al. (2016) carefully checked these sources and provided a homogenous sample of 172 open clusters with metallicity (and also age) adjusted to a consistent scale. This is our primary sample. Meanwhile, Soubiran et al. (2018) provided accurate radial velocities for 861 open clus-

ters and calculated Galactic velocities based on these radial velocities, the most probably distances and proper motions in Cantat-Gaudin et al. (2018) from *Gaia* DR2 (Gaia Collaboration et al. 2018a,b). The primary sample from Netopil et al. (2016) is cross-matching with the kinematic sample of Soubiran et al. (2018) and we obtain a sample of 148 open clusters.

Fig. 1 shows the metallicity gradient and the age-metallicity relation for this sample. Metallicities derived by different ways are marked by different symbols: photometrical indices (126 open clusters; dots), high-resolution (80 open clusters; red open circles) and low-resolution (39 open clusters; blue open circles) spectroscopic data. It shows that metallicities from high-resolution spectroscopic data have smaller scatters in metallicity than those from low-resolution spectroscopic data and photometrical indices at a given Galactic radial distance. Among 148 open clusters in this sample, we adopt metallicities from high-resolution spectroscopic data for 80 open clusters, from low-resolution spectroscopic data for 10 open clusters and from photometric indices for the remaining 58 open clusters. The error in metallicity is about 0.06 dex according to Netopil et al. (2016).

The sample covers a metallicity range of $-0.50 < [\text{Fe}/\text{H}] < +0.43$, an age range of $0.01 < t < 7.79$ Gyr and a Galactic radial distance range of $5 < R < 15$ kpc. Two exceptional open clusters, Berkeley 22 at 18.1 kpc and Berkeley 29 at 27.1 kpc, are excluded from this sample because at such farther radii they do not follow the general metallicity gradient (i.e. the decreasing $[\text{Fe}/\text{H}]$ trend with increasing R), which is required for estimating the birth site. Thus, our final sample includes 146 open clusters for further analysis. This sample has advantage to probe the role of radial migration at the early stage of the evolution of the Galactic disk because the majority of open clusters are quite young. Meanwhile, this sample has a wide span until 8 Gyr with 50 clusters older than 1 Gyr, and thus it is still a good sample for probing the age effect of radial migration on the Galactic disk.

3 ANALYSIS

3.1 The birth site: R_b

The birth sites are calculated based on the relation of $R_b - R_\odot = ([\text{Fe}/\text{H}]_{OC} - [\text{Fe}/\text{H}]_{ism}(R_\odot, t)) / \text{gradient}(t)$, where t represents age of open cluster and R_\odot is the solar radius of 8.34 kpc (Reid 2014) used in the present work. The ISM metallicity at solar radius and the metallicity gradient as functions of age are taken from Minchev et al. (2018). Ages and metallicities of open clusters by Netopil et al. (2016) are adopted. The error in the calculated birth site is based on uncertainties of metallicity and age by the bootstrap method (1000 times for each cluster). As shown in Fig. 2, the error distribution of the birth site has a peak at ~ 0.1 kpc with an extended tail toward 1 kpc. This is an internal uncertainty and it is expected that the external error could be larger. In Fig. 3, open clusters with $t < 2.5$ Gyr at solar radius are compared with the ISM profile of Minchev et al. (2018), and the metallicity gradient of very young clusters with $0.1 < t < 0.5$ Gyr is of

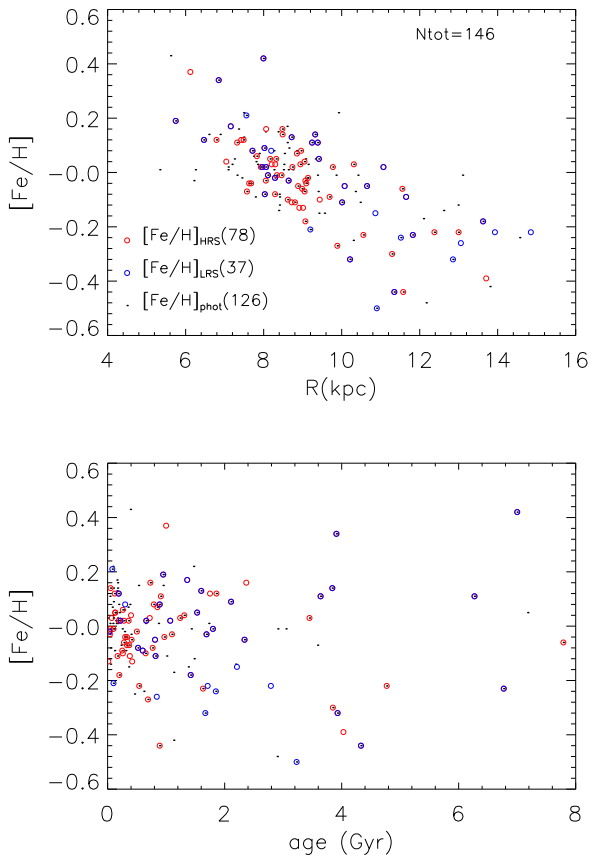


Figure 1. The metallicity gradient and the age-metallicity relation for of the selected sample of 146 open clusters. Metallicities from high-resolution spectroscopic data (78/80; red open circles), low-resolution spectroscopic data (10/39; blue open circles) and photometric indices (58/126; black dots) are indicated separately.

-0.07 dex/kpc . It shows that there is no systematic shift in the metallicity scale between our sample and the HARPS data of Minchev et al. (2018), although there is a substantial scatter in metallicity for young open clusters. Meanwhile, the present gradient from very young clusters with $0.1 < t < 0.5 \text{ Gyr}$ is exactly the same as the value used in Minchev et al. (2018).

Fig. 4 shows the birth sites R_b versus $[\text{Fe}/\text{H}]$ for five age ranges, $t < 0.5 \text{ Gyr}$, $t = 0.5 - 1.0 \text{ Gyr}$, $t = 1.0 - 2.5$, $t = 2.5 - 5.0 \text{ Gyr}$ and $t > 5.0 \text{ Gyr}$. The birth site R_b covers a wide range of $0 - 15 \text{ kpc}$, as large as the whole R range. Here, Galactic radial distance is of $R = \sqrt{X * X + Y * Y}$. Four super metal rich ($[\text{Fe}/\text{H}] > 0.2$) clusters come from the inner disk ($R_b < 5 \text{ kpc}$) and five metal poor ($[\text{Fe}/\text{H}] < -0.4$) clusters from the outer disk ($R_b > 13 \text{ kpc}$). It seems that the main factor that determines R_b is of metallicity. and the second factor of age.

In Fig. 5, the excursion distance, $(R - R_b)$, varies from -4 kpc to $+7 \text{ kpc}$, and it increases generally with age (and also with metallicity). Specifically, $(R - R_b)$ is negative at $\sim -2 \text{ kpc}$ for young clusters with $t < 0.5 \text{ Gyr}$, while it becomes positive with $(R - R_b) \sim +4 \text{ kpc}$ for the oldest age bin of $t > 5 \text{ Gyr}$ in our sample. Five exceptional clusters, NGC

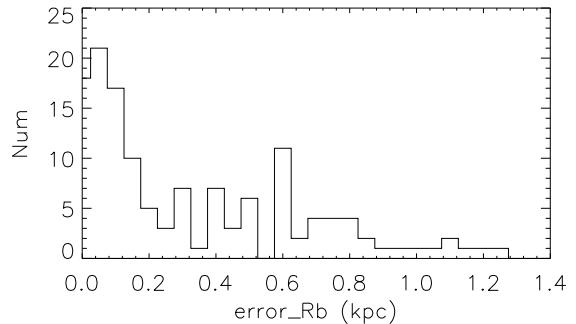


Figure 2. The error distribution of the birth site R_b in this sample.

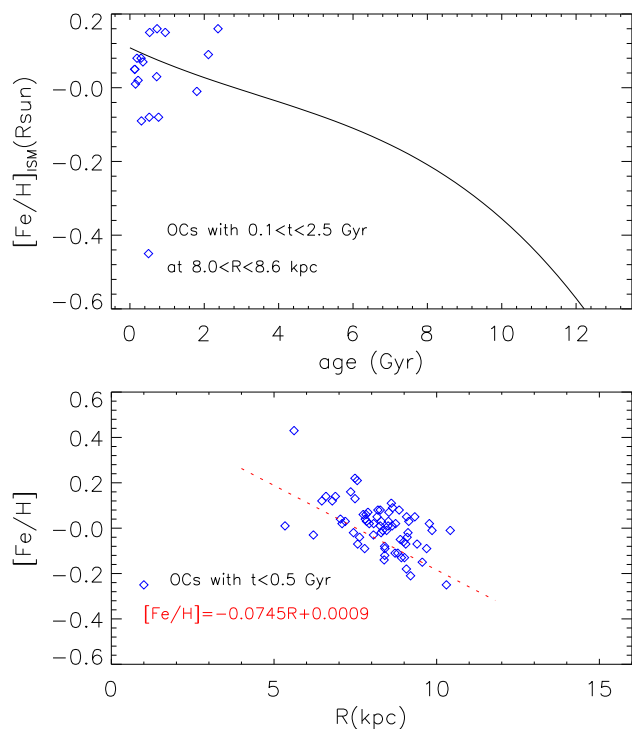


Figure 3. Upper: The evolution of ISM metallicity at solar radius from Minchev et al. (2018) (black line) with overlaid open clusters with $t < 2.5 \text{ Gyr}$ at solar radius (blue diamonds). Lower: The present metallicity gradient is of -0.07 dex/kpc (red dash line) derived from very young clusters with $0.1 < t < 0.5 \text{ Gyr}$ (black crosses).

2243, Berkeley 99, Trumpler 5, Melotte 66 and Berkeley 32, do not follow the general trend in the $(R - R_b)$ versus age diagram. They have intermediate ages of $3 - 4 \text{ Gyr}$ but with the lowest metallicity of $[\text{Fe}/\text{H}] < -0.4$.

There is a weakly increasing trend of the excursion distance $(R - R_b)$ toward the outer disk as shown in Fig. 6. This positive $(R - R_b)$ at $R > 12 \text{ kpc}$ is in agreement with the results of Reddy et al. (2016) who suggested that the outer disc clusters were actually born inward and radial migration

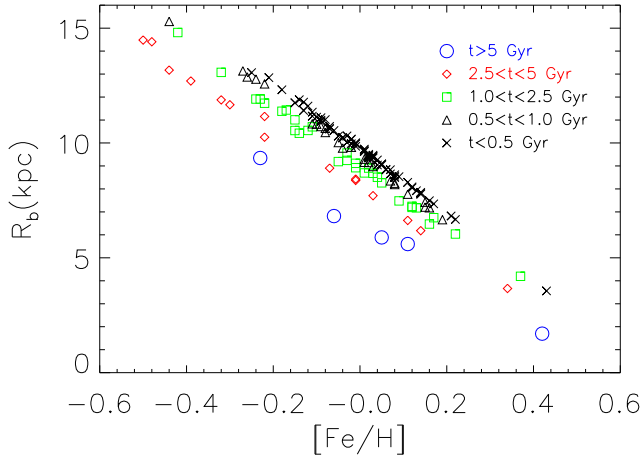


Figure 4. The birth site R_b versus $[\text{Fe}/\text{H}]$ for five age intervals, $t < 0.5$ Gyr (black crosses), $0.5\text{--}1.0$ Gyr (black triangles), $1.0\text{--}2.5$ Gyr (green squares), $2.5\text{--}5$ Gyr (red diamonds) and $t > 5$ Gyr (blue open circles).

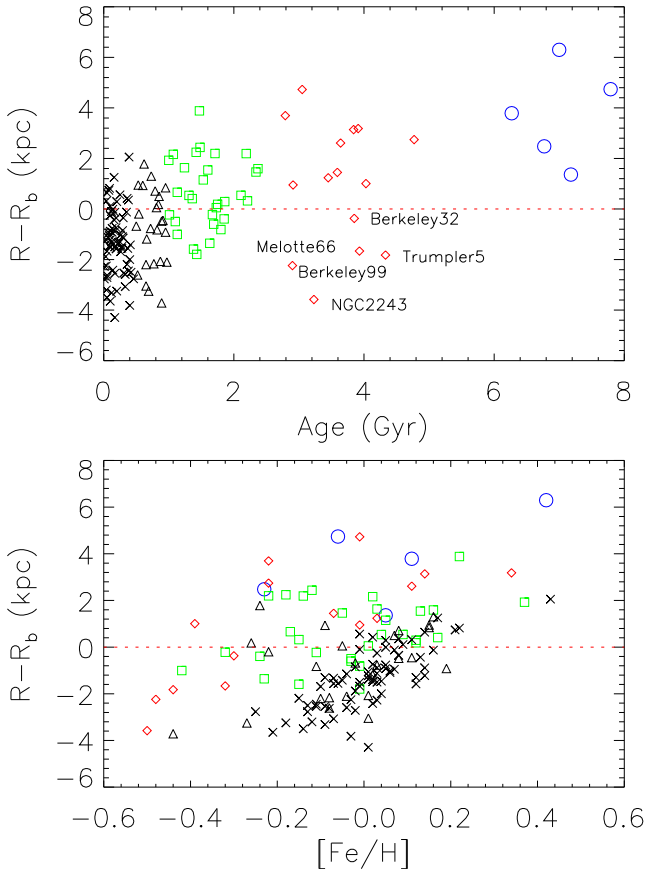


Figure 5. The excursion distance $R - R_b$ as functions of metallicity and age. The symbols are same as in Fig. 4.

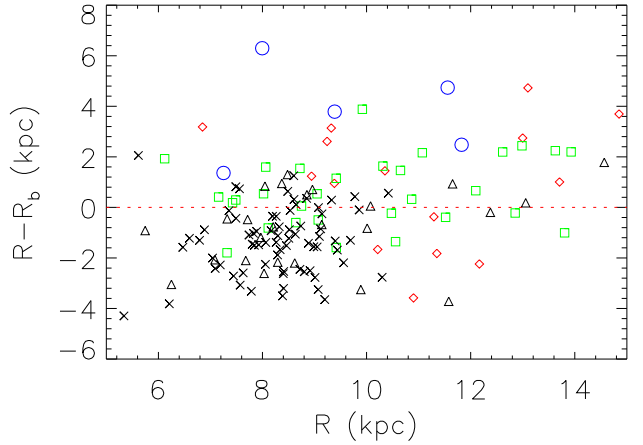


Figure 6. The excursion distance $R - R_b$ as functions of Galactic radial distance. The symbols are same as in Fig. 4.

had taken them to present locations. Meanwhile, there is an age difference between the solar circle and the outer disk clusters. Young clusters with $t < 0.5$ Gyr covers a R range of $6 - 10$ kpc but old open clusters span a wider R range from the inner disk toward the outer disk at $10 - 15$ kpc. The relative number of old versus young clusters increases with Galactic radius, which indicates an increase of outward migrators toward the outer disk where old clusters should be formed first and inside (under the assumption of the inside-out formation) and then migrated to the outer disk. This supports the theoretical simulation work by [Minchev et al. \(2014\)](#), who suggested that there should be an increase in the relative number of outward migrators with Galactic radius.

3.2 Orbital parameters: R_m and R_g

The metallicity versus Galactic radial distance is shown for the five age bins in Fig. 7. It is clear that young open clusters with $t < 0.5$ Gyr have lower average $[\text{Fe}/\text{H}]$ than those with $0.5 < t < 2.5$ Gyr and $t > 2.5$ Gyr. According to [Netopil et al. \(2016\)](#), at $7 < R < 9$ kpc, the metallicity of old open clusters with $1.0 < t < 2.5$ Gyr is 0.06 dex higher than that of young ones with $t < 0.5$ Gyr in their cleaned sample. They suggested that the increase of metallicity with age can be explained by radial migration and this was supported by theoretical simulations of [Minchev et al. \(2013\)](#) and [Grand et al. \(2015\)](#). That is, higher metallicity of old open clusters with $1.0 < t < 2.5$ Gyr were born in the more metal rich inner regions and migrate outward to present location.

This direct comparison of average metallicity at a given Galactic location does not work for older open clusters, i.e. $2.5 < t < 5.0$ Gyr and $t > 5.0$ Gyr, since there are only a few such clusters and they locate at different R ranges. Instead, the comparison between the birth site and orbital parameter provides a good way to evaluate the effect of radial migration. For this purpose, we calculate the orbital parameters, peri-center/apo-center distances R_p , R_a and guiding radius R_g for the sample based on the axis-symmetric potential MWPotential2014 with the publicly available pack-

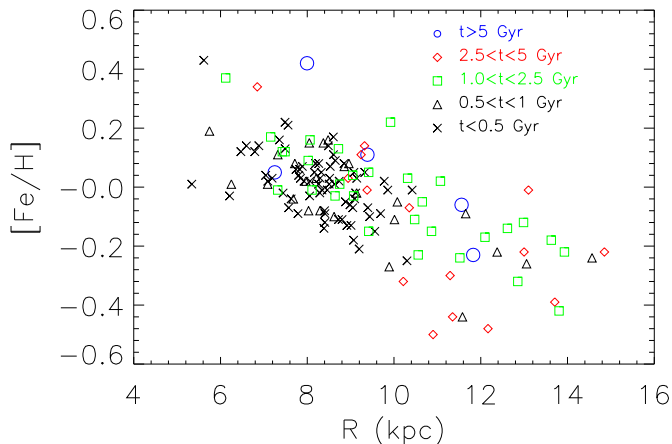


Figure 7. The $[\text{Fe}/\text{H}]-R$ for different age bins. The symbols are same as in Fig. 4.

age *Galpy* by Bovy (2015). Here we adopt the solar radius of 8.34 kpc and the circular velocity of 238 km/s presented by Reid (2014).

In order to investigate the blurring effect of the Galactic disk, we show how different these orbital distances deviate from Galactic radial distance R and how these deviations vary with Galactic locations. Fig. 8 shows the $R_m - R$ and $R_g - R$ versus R , where the mid-point distance is defined to be $R_m = (R_a + R_p)/2.0$. For young open clusters with $t < 0.5$ Gyr, $R_m - R \sim +1$ kpc and most open clusters with $t < 2.5$ Gyr locate within a limited range of 1.5 kpc around the mean value of 1.0 kpc. But a few old open clusters at $R > 10$ kpc have large $R_m - R$ values (3–5 kpc). Among 146 open clusters, 14 of them have $|R_g - R| > 1$ kpc and they are found to have excursed at a distance of ~ 2 kpc. That is, about 10% open clusters have guiding radii quite different from present locations as a result of the blurring process. 90% open clusters have $|R_g - R| < 1$ kpc, for which radial excursions from their guiding radii to present locations are not significant. Moreover, we note that almost all clusters with $t < 2.5$ Gyr lie within $|R_g - R| < 1$ kpc, while clusters showing $|R_g - R| > 1$ kpc are all older than 2.5 Gyr. It seems that the blurring effect requires a timescale of 2.5 Gyr to stray to a distance of larger than 2 kpc from the guiding radius. Finally, we notice that these clusters locate mainly at $R > 10$ kpc, which indicates that the blurring effect favors to work outside the solar circle, e.g. at 10–15 kpc. In consistent with this suggestion, Fig. 9 shows that open clusters undergoing large excursion ranges of $R_a - R_p > 5$ kpc also occur in the outer disk beyond 10 kpc.

From Fig. 8, it seems that R_g may be a better representative for orbital distance than R_m because R_g is quite close to R and R_p for young open clusters with $t < 2.5$ Gyr, while R_m shows a systematic shift of 1 kpc from R even for very young open clusters with $t < 0.5$ Gyr. Moreover, since R_g is directly related with the angular momentum by definition, it is a good proxy for current orbital distance to investigate the churning effect of radial migration in the following analysis. When R is replaced by R_g in the X-axis of Fig. 7, it is found, in Fig. 9, that the metallicity seems to decrease continuously with R beyond $R_g > 12$ kpc, which makes it

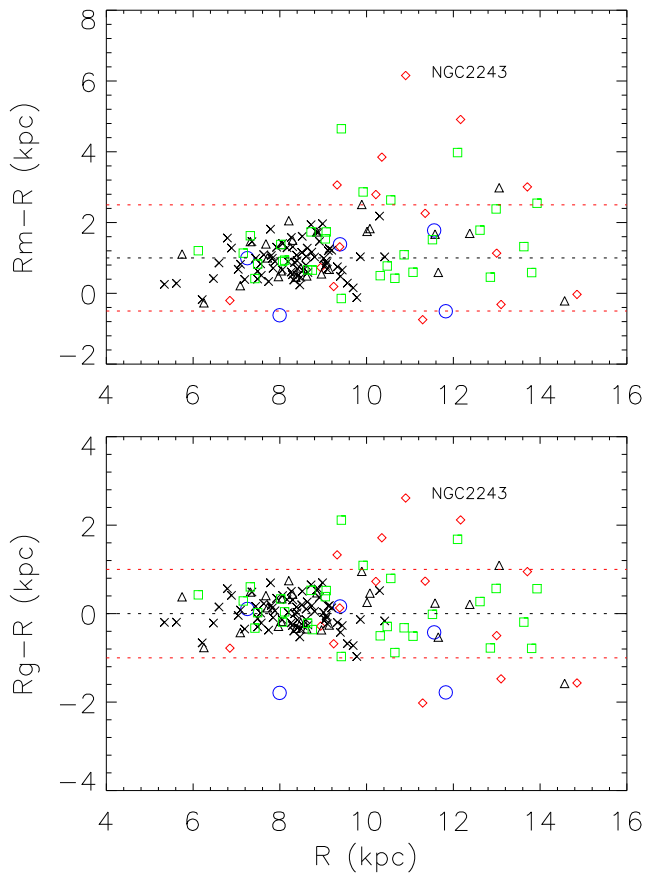


Figure 8. The $R_m - R$ and $R_g - R$ versus R for different age bins. The symbols are same as in Fig. 4.

plausible for us to estimate the birth site for open clusters with $R > 12$ based on a single metallicity gradient. The decreasing metallicity with R was also found for Cepheid variables by Luck & Lambert (2011) and it is valid until $R \sim 15$ kpc, which is the high limit of our sample. In addition, the dispersion of $[\text{Fe}/\text{H}]$ at a given R_g is somewhat reduced for the outer disk beyond 12 kpc. All these results show that R_g is a good proxy for current orbital distance.

3.3 The migration distance versus age diagram

The migration distance, $R_g - R_b$, is a representative value to estimate the effect of the churning process of radial migration. Note that R_b is calculated from metallicity and age, while R_g is related with the kinematic parameter, the circular velocity. Thus, the migration distance, $R_g - R_b$, has the advantage to combine the metallicity, kinematics and age information, which is important for tracing the evolution of the Galaxy. Fig. 11 shows $R_g - R_b$ versus age for four R ranges, $5 < R < 7$ kpc, $7 < R < 9$ kpc, $9 < R < 12$ kpc and $12 < R < 15$ kpc. The upper panel is for the whole age range and the lower panel shows the enlarged part in the low age range of $t < 2.5$ Gyr. In general, young open clusters with $t < 1.0$ Gyr migrate inward with negative $R_g - R_b$ values, while older clusters with $t > 1.0$ Gyr usually migrate outward with positive values. The increasing trend of $R_g - R_b$

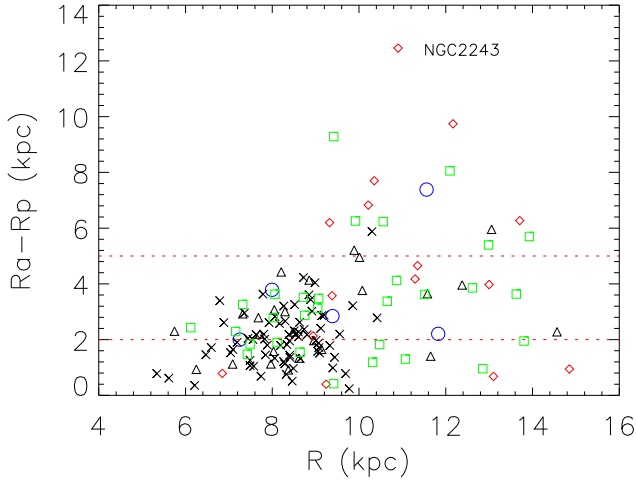


Figure 9. The $R_a - R_p$ versus R for different age bins. The symbols are same as in Fig. 4.

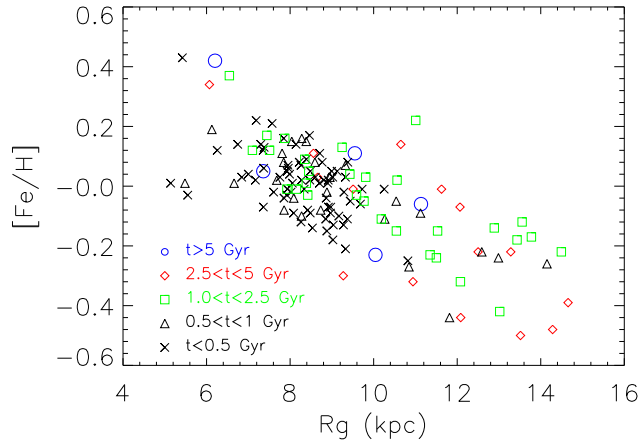


Figure 10. The $[\text{Fe}/\text{H}]$ versus R_g for different age bins. The symbols are same as in Fig. 4.

with age is seen for young clusters with $t < 2.5$ Gyr and extends for the whole age range we investigated. This provides a supportive evidence on the role of radial migration, which requires time for clusters to stray from their birth sites to the present positions, and thus older clusters tend to have larger migration distances.

However, at all ages, there are open clusters with $R_g - R_b$ near zero (within 1 kpc); they do not experience significant churning process. Thus, it needs a more specific inspect on how different radial migration (or churning) works on individual clusters. In the upper panel of Fig. 11, the black solid line separates open clusters move inward and outward, while the red solid line shows the migration distance that can be reached during its lifetime assuming a migration rate of $1 \text{ kpc}/\text{Gyr}$ (see Chen et al. 2019 for details). Taking into account of the maximum error of 1 kpc in R_b , we shift the red solid upward by 1 kpc (the dash red line) and the two black dash lines are drawn within 1 kpc around the black solid line. In this way, we define four regions in Fig. 11: Region A above the red solid line, Region B below the red line and above the upper black dash line, Region C

within the two black dash lines, and Region D below the lower black dash line.

There are 16 open clusters at Region A with six of them (NGC 6583, NGC 6603, Pismis 2, NGC 1798, Berkeley 73 and IC 166) above the red dash line. They move outward from their birth sites to present locations, but the migration distance is larger than the reachable distance within their lifetimes under the assumption of a migration rate of 1 kpc per Gyr. However, the migration rate may be as large as $1.5 \text{ kpc}/\text{Gyr}$ at the outer disk as we will show later, which makes it easier for radial migration to account for clusters at Region A. Meanwhile, we notice that the blurring effect may also play a significant role for some clusters at this region. For example, IC 166 has $R_g - R = 1.67$ kpc and Pismis 2 has $R_g - R = 1.09$ kpc. Since most clusters at Region A locate within the red dash line, it seems that radial migration generally accounts for their origins.

Old open clusters with $t > 2.5$ Gyr mainly locate at Region B, where the well known old metal rich cluster, NGC 6791, is a typical case. Due to their large ages, radial migration definitely accounts for the migration distances of these open clusters under the assumption of $1 \text{ kpc}/\text{Gyr}$ migration rate. The migration distance varies greatly for old clusters, such as Collinder 261 and NGC 6791 as shown in Fig. 11. Thus, age is not the only factor that determines the migration distance.

Open clusters at Region C are defined to have migration distances around zero (within 1 kpc); they do not experience significant radial migration. Most clusters at Region C have ages less than 5.0 Gyr with only one exception (Berkeley 39). Berkeley 39 at $R = 11.8$ kpc has $t \sim 7$ Gyr and the migration distance of $R_g - R_b \sim 1$ kpc, significantly lower than that of NGC 6791 at similar age. The existence of Berkeley 39 indicates that the outer disk has locally-born old cluster, which is unusual under the assumption of the inside-out formation scenario.

In Region D, most clusters are younger than 1 Gyr with one exception (Berkeley 32, 4 Gyr at $R = 11.3$ kpc). The migration distance in this region covers a wide range of 4 kpc from $R_g - R_b = -5$ kpc to -1 kpc. They locate within 12 kpc (with one exception, Berkeley 23 at $R = 13.8$ kpc) where the metallicity gradient is valid. Finally, we note that the clusters from inner disk ($R < 7$ kpc) have the largest span in migration distance from the lowest to the highest values, although they are all younger than 1 Gyr (with one exception, NGC 6253 with $t = 3.91$ Gyr and $[\text{Fe}/\text{H}] = 0.34$ dex).

3.4 The migration rate

With the migration distance and age, it is possible to estimate a rough migration rate as defined to be the division of the migration distance over the cluster's age. Fig. 12 shows the distributions of the migration rate for open clusters with $t > 0.1$ Gyr as a function of age. Very young open clusters with $t < 0.1$ Gyr should be excluded since very small value in age would lead to a very large and uncertain migration rate. For young clusters with $t < 1.0$ Gyr, the migration rate varies from $-5.0 \text{ kpc}/\text{Gyr}$ to $+2.5 \text{ kpc}/\text{Gyr}$, a wide range of $7.5 \text{ kpc}/\text{Gyr}$. The upper envelope of migration rate is of $+2 \text{ kpc}/\text{Gyr}$ for intermediate-age clusters with $1.0 < t < 3.0$ Gyr and it seems to decrease to $0.5 - 1.0 \text{ kpc}/\text{Gyr}$ for the

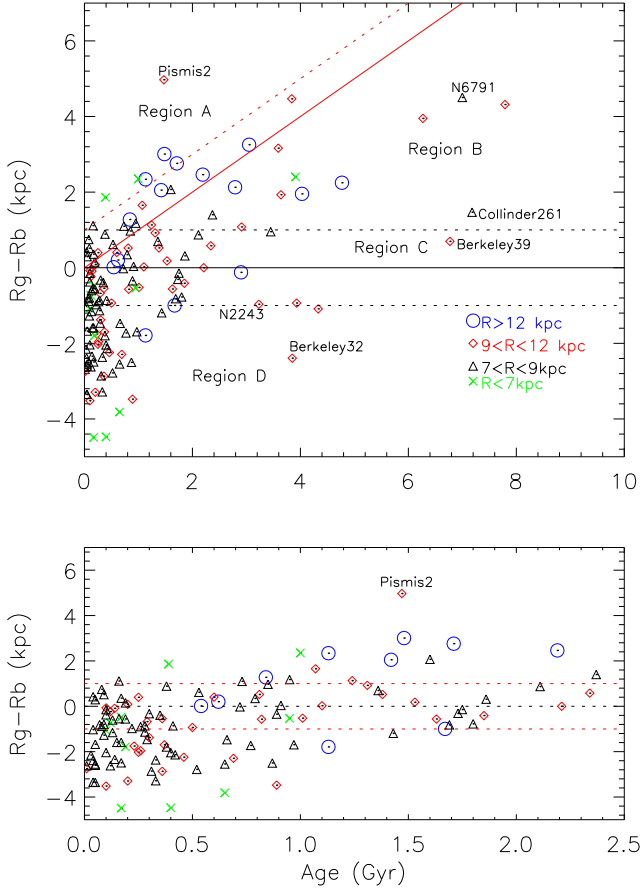


Figure 11. The $R_g - R_b$ versus age diagram for open clusters at different R ranges: $5 < R < 7$ kpc (green crosses), $7 < R < 9$ kpc (black triangles), $9 < R < 12$ kpc (red diamonds) and $R > 12$ kpc (blue circles). Lower panel shows the enlarged part of 0 – 2.5 Gyr.

oldest ones with $5 < t < 8$ Gyr. In general, the histogram of the migration rate shows a peak at zero, since 64 clusters (out of 146) in our sample do not experience radial migration with $|R_g - R_b| < 1$ kpc. For clusters moving outward ($R_g - R_b > 1$ kpc), the peak of the migration rate is of $0.5 - 1.5$ kpc/Gyr, while there is a wide distribution from -5 kpc/Gyr to -1 kpc/Gyr for inward-moving clusters with $R_g - R_b < -1$ kpc.

However, the above-defined migration rate might represent a low limit for old clusters because we do not know the exact time span of the migration process. According to Minchev et al. (2011), radial migration starts from 0.4 Gyr and continues until 3.0 Gyr or longer (see their Fig. 1), which might indicate a time span of $\sim 2.5 - 3.0$ Gyr. In view of this, the most plausible way to estimate the migration rate in the present work is based on intermediate-age outer-disk clusters, since they have experienced a larger migration distance than those from the solar circle and their ages are comparable to the time span of the migration process. Thus, we select open clusters with intermediate-age of $0.5 < t < 3.5$ Gyr and at the outer disk of $12 < R < 15$ kpc and we obtain a migration rate of $\sim 1.5 \pm 0.5$ kpc/Gyr, as shown by the red solid line in the low panel of Fig.

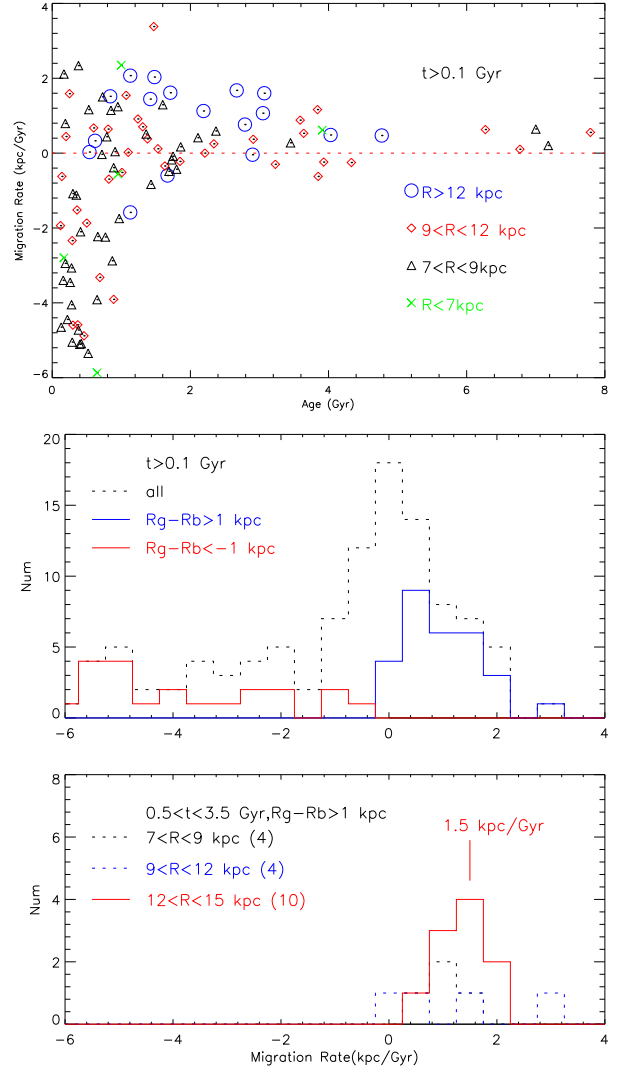


Figure 12. Upper: The estimated migration rate versus age for all open clusters with $t > 0.1$ Gyr (dash black line) at four R ranges with the same symbols as in Fig. 11. Middle: The histograms of the migration rate for migrated clusters moving outward ($R_g - R_b > 1$ kpc; blue solid line) and inward ($R_g - R_b < -1$ kpc; red solid line), as well as for all clusters with $t > 0.1$ Gyr (dash black line). Lower: The migration rate is measured to be $\sim 1.5 \pm 0.5$ kpc/Gyr based on intermediate-age clusters ($0.5 < t < 3.5$ Gyr) at the outer disk ($12 < R < 15$ kpc). For comparison, the histograms from clusters at $9 < R < 12$ kpc (blue dash line) and $7 < R < 9$ kpc (black dash line) are also shown.

12. At the same age range, four clusters at the solar circle show a peak of migration rate at ~ 1.0 kpc/Gyr. These values are consistent or slightly larger than our adopted value of 1 kpc/Gyr from Quillen et al. (2018), who estimated the migration rate based on the Gaussian bar model by Comparetta & Quillen (2012). This consistency shows the important role of the Galactic bar in the theoretical modeling of radial migration process, as already included in the chemical-dynamical model by Minchev et al. (2013).

4 IMPLICATIONS ON THE MECHANISMS OF RADIAL MIGRATION AND ITS ROLE ON THE GALACTIC DISK

Since open clusters belong to the young population of the Galactic disk, it is expected that they do not suffer from significant radial excursions caused by the blurring process, which is favored by the old population. It is found that 90% open clusters have $|R - R_g| < 1$ kpc, which indicates that the blurring effect do not play a significant role for this young population of the Galactic disk. However, only 44% (64 out of 146) open clusters with $|R_g - R_b| < 1$ kpc do not suffer from significant churning process as shown in the migration distance versus age diagram. The remaining 56% clusters have a wide range of absolute migration distance ($|R_g - R_b|$) from 1 – 5 kpc for all ages. Those migrated clusters provide unique and valuable insights on the mechanisms of radial migration in the Galactic disk.

One of the most interesting result in the present work may be that the migrated open clusters have different behaviors in migration direction. 53 clusters with $R_g - R_b < -1$ kpc at Region D migrate inward, while 29 clusters with $R_g - R_b > 1$ kpc migrate outward, among which 13 can be explained by the churning process alone and 16 need other mechanisms working together. As shown in Fig. 11, where the inward-migrated clusters with $R_g - R_b < -1$ kpc are younger than 1.0 Gyr (the young group), while the outward-migrated clusters with $R_g - R_b > 1$ kpc are older than 1.0 Gyr (the old group). Moreover, the migration rates vary greatly in the young group and there are more consistent values around $1 - 1.5$ kpc/Gyr for the old group. Finally, the outward-migrated clusters mainly belong to the outer disk with $R > 9$ kpc (and dominate at $R > 12$ kpc), while the inward-migrated clusters have $R < 12$ kpc and dominate at the solar circle of $7 < R < 9$ kpc. These differences between the young and old groups among these migrated clusters may indicate their different theoretical mechanisms of radial migration.

The migrated clusters in the old group may be explained by the coupled model of the bar and spiral arms of [Minchev et al. \(2013\)](#). They show a relatively constant migration rate of $\sim 1.5 \pm 0.5$ kpc/Gyr, which is generally consistent with the migration rate of 1 kpc/Gyr presented in [Quillen et al. \(2018\)](#) for a pitch angle of 24 based on the Gaussian bar model by [Comparetta & Quillen \(2012\)](#). Meanwhile, super metal rich stars detected in the LAMOST survey by [Chen et al. \(2019\)](#) also favor the model by [Minchev et al. \(2013\)](#). In this respect, NGC 6791 is a typical case as the most metal-rich ($[\text{Fe}/\text{H}] = 0.37$) but quite old ($t = 7.0$ Gyr) cluster ([Netopil et al. 2016](#)). It has thick disk kinematics locating at $R = 6.1$ kpc and $|Z| = 0.87$ kpc. [Linden et al. \(2017\)](#) suggested that it is unlikely for a radial migration mechanism to operate by several kpc, and especially to account for the current cluster's high altitude above the plane. However, [Martinez-Medina et al. \(2017\)](#) found that a fraction of the newly formed clusters would eventually migrate more than 4 kpc and be lifted up to 0.8 kpc above the disk's mid-plane. In their simulation, abundant examples of orbits supported the scenario that NGC 6791 started their evolution in the inner disk and reached to the present location by radial migration. Our results also

suggest that radial migration accounts for its orbital parameters, migration distance and Galactic location.

For the young group, Theoretical works by [Fujii et al. \(2012\)](#) might provide some hints on their migration mechanism. According to their simulation, star clusters in non-steady disks lose or gained angular momentum, and they could migrate inward or outward by the order of a few kpc in a few hundred Myr. The existence of very young clusters ($t < 0.3$ Gyr) in Fig.12 provides observational support on this simulation. Moreover, it seems that the migration rate is not constant but varies greatly from -6 kpc/Gyr to zero. But further works on the theoretical mechanisms, radial migration or other scenarios, are necessary to explain the behaviors of these very young open clusters with $t < 1.0$ Gyr.

5 SPECIAL CLUSTERS AT THE GALACTIC OUTER DISK

The Galactic outer disk is significantly influenced by both the blurring process (10% clusters with $|R - R_g| > 1$ kpc showing $R_g > 10$ kpc) and the churning process (with a high migration rate of 1.5 ± 0.5 kpc/Gyr). Moreover, [Quillen et al. \(2009\)](#) and [Bird, Kazantzidis & Weinberg \(2012\)](#) suggested that perturbations caused by minor mergers are effective at mixing the outer disks of galaxies. Thus, it is expected that the Galactic outer disk has a complicate history, which might be seen from some special clusters in the sample.

NGC2243 is one of the most special cluster in our sample due to the lowest metallicity of $[\text{Fe}/\text{H}] = -0.5$, the highest Z_{max} of 2.65 kpc, the farthest apo-center distance of 23.3 kpc and the highest eccentricity of 0.37. The high rotation of $V_\phi = 278.3$ km/s derived in this work and low α abundances from [Francois et al. \(2013\)](#) indicate its origin from the thin disk population. Its present location is far from R_g , R_m and has the largest excursion range of $R_a - R_p$ of 12.7 kpc. The highest eccentricity of 0.37 is consistent with the significant effect of the blurring process, while churning does not work as indicated by the $|R_g - R_b| < 1$ kpc. The large $R_a = 23.3$ kpc and high $Z_{max} = 2.65$ kpc may suggest that minor mergers also work in this intermediate-age cluster. According to [Minchev et al. \(2014\)](#), the impact of mergers is the largest in the outer disks of galaxies due to the lower potential.

Pismis 2 has a typical thin-disk kinematics. The high metallicity of $[\text{Fe}/\text{H}] = 0.22$ at the outer disk of $R_g = 11.0$ makes it a special case, since most stars at this radius is metal poor with $[\text{Fe}/\text{H}] \sim -0.4$. The high metallicity indicates a small birth radius from the inner disk, which leads to the largest migration distance of $R_g - R_b = 4.97$ kpc in our sample. Based on its age of 1.47 Gyr, the migration rate is around 3.4 kpc/Gyr, the highest one among the old group of migrated clusters. It is not consistent with the values based on either other clusters at the outer disk (1.5 kpc/Gyr). The blurring effect is not significant with $R - R_g = 1.08$ kpc, and its eccentricity of 0.25 and low $Z_{max} = 0.5$ kpc do not favor for the scenario of minor mergers. Further study on mechanisms of the churning process is desirable to explain its high migration distance.

Berkeley 39 has a thick-disk kinematics, high $Z_{max} =$

1.36 kpc and old age of 8.0 Gyr. All of these indicates that it belongs to the thick disk population. The suggestion is further supported by its enhanced $[\alpha/\text{Fe}]$ ratios based on $[\text{Mg}/\text{Fe}]$, $[\text{Al}/\text{Fe}]$ and $[\text{Si}/\text{Fe}]$ abundances derived from four giants by Friel et al. (2010). It has a low eccentricity of $e = 0.1$ and travels within 2 kpc between $R_p = 10.2$ kpc and $R_a = 12.4$ kpc. It is unlikely that the blurring process or minor mergers works. Finally, $R_g - R_b$ is less than 1 kpc, which further excludes the contribution from the churning process. Thus, it is a locally-born old thick disk cluster at the outer disk.

In addition, there are other special clusters at the outer disk. For example, Berkeley 23 (at $R = 13.8$ kpc) is the only cluster at the outer disk that migrates inward. It has $[\text{Fe}/\text{H}] = -0.42$ and $t = 1.1$ Gyr with a migration rate of 1.7 kpc/Gyr, a typical value for the outer disk. Its metallicity is typical at its Galactic radius and its young age makes it special for the outer disk. On contrary, Berkeley 32 at $R = 11.2$ kpc is 4-Gyr-old cluster that migrated inward. Both the blurring and churning effects works together, and its low eccentricity does not favor for the scenario of minor mergers. The existence of different kinds of special clusters indicates a complicated formation history of the Galactic outer disk.

6 CONCLUSIONS

A homogenous sample of 146 open clusters with available metallicity, age, velocities and orbital parameters is obtained by cross-matching the scaled metallicity/age catalog of Netopil et al. (2016) and accurate kinematic catalog of Soubiran et al. (2018) based on Gaia DR2. This sample spans a metallicity range of -0.5 to $+0.4$ dex, a range in age of a few Myr to 8 Gyr and a range of 5 to 15 kpc in radial radius. It allows us to explore the role of radial migration on the Galactic disk by interpreting Galactic locations, orbital parameters of open clusters and their migration distances as a function of age.

The comparison of present location with orbital parameters, R_m and R_g , shows that 90% open clusters have $|R_g - R| < 1$ kpc and $|R_m - R| = 1 \pm 1.5$ kpc. Meanwhile, 10% clusters with $|R_g - R| > 1$ kpc and $R_m - R > 2.5$ kpc mainly locate at the outer disk of $R > 10$ kpc. This indicates that blurring causes significant radial excursions for only 10% open clusters in our sample, mainly at the outer disk.

The birth sites of open clusters are calculated, and the deviation between the guiding distance and the birth site ($R_g - R_b$) corresponds to the churning process of radial migration. In our sample, 56% open clusters suffer from significant churning and they move in two opposite directions. Young clusters with $t < 1.0$ Gyr migrate inward by 2–5 kpc, while old clusters with $t > 1.0$ Gyr migrate outward by 2–4 kpc. The large migration distances of young open clusters supports theoretical simulation by Fujii et al. (2012), which suggested that the migration of several kpc could happen within a few Myr. For older clusters, the chemo-dynamical evolution model by Minchev et al. (2013) is the most favorite mechanism, which successes to explain their distributions in the migration distance versus age diagram. Based on intermediate-age clusters at the outer disk, we measure

the migration rate of 1.5 ± 0.5 kpc/Gyr, which is consistent with the prediction of 1 kpc/Gyr by Quillen et al. (2018) for a pitch angle of 24 based on the Gaussian bar model by Comparetta & Quillen (2012).

Finally, we find several special clusters at the outer disk, a thin-disk cluster (NGC 2243) with the merging history excusing out to 23 kpc, a metal-rich outer disk cluster (Pismis 2) with the largest migration distance of 4.97 kpc, and a locally-born old thick-disk cluster (Berkeley 39). The existence of different kinds of special clusters implies a complicated formation history of the outer disk of our Galaxy.

ACKNOWLEDGEMENTS

We would like to thank the referee for his valuable suggestions, which greatly improve the manuscript.

This study is supported by the National Natural Science Foundation of China under grant Nos. 11988101, 11625313, 11890694 and the National Key R & D program of China of 2019YFA0405502.

This work has made use of data from the European Space Agency (ESA) mission *Gaia* (<https://www.cosmos.esa.int/gaia>), processed by the *Gaia* Data Processing and Analysis Consortium (DPAC, <https://www.cosmos.esa.int/web/gaia/dpac/consortium>). Funding for the DPAC has been provided by national institutions, in particular the institutions participating in the *Gaia* Multilateral Agreement.

REFERENCES

- Anders, F., et al., 2017, *A&A*, 600, A70
 Reddy A.B.S., Lambert D.L., & Giridhar S., 2016, *MNRAS*, 463, 4366
 Bird, J.C., Kazantidis, S. & Weinberg, D.H. 2012, *MNRAS*, 420, 913
 Bovy, J. 2015, *ApJS*, 216, 29
 Cantat-Gaudin, T., Jordi, C., Vallenari, A., et al. 2018, *ArXiv e-prints* [arXiv:1805.08726]
 Casagrande, L., Schönrich, R., Asplund, M., et al. 2011, *A&A*, 530, A138
 Chen, Y.Q.; Zhao, G.; Zhao, J.K. et al. 2019, *AJ*, 245, 216
 Comparetta, J. & Quillen, A. C. 2012, *astro-ph/1207.5753*
 Dias, W. S., Alessi, B. S., Moitinho, A., & Lépine, J. R. D. 2002, *A&A*, 389, 871
 Edvardsson, B.; Andersen, J.; Gustafsson, B. et al. 1993, *A&A*, 275, 101
 Frankel, Neige; Rix, Hans-Walter; Ting, Yuan-Sen et al. 2018, *ApJ*, 865, 96
 Francois, Franois, P.; Pasquini, L.; Biazzo, K.; Bonifacio, P.; Palsa, R. 2013, *A&A*, 552, A136
 Friel, E. D., Jacobson, H. R., & Pilachowski, C. A., 2010, *AJ*, 139, 1942
 Fujii, M.S. & Baba, J. 2012, *MNRAS*, 427, 16
 Grand, R. J. J.; Kawata, D. & Cropper, M. 2015, *MNRAS*, 447, 4018
 Grand, R. J. J.; Kawata, D. 2016, *AN*, 337, 957
 Grenon, M., 1972, in Cayrel de Strobel G., Delplace A. M., eds, *IAU Colloq. 17: Age des Etoiles*. p. 55
 Hayden, Michael R.; Bovy, Jo; Holtzman, Jon A. et al. 2015, *ApJ*, 808, 132
 Haywood, M. 2008, *MNRAS*, 388, 1175

- Haywood, Misha; Di Matteo, Paola; Lehnert, Matthew D. et al. 2013, *A&A*, 560, 109
- Feltzing, S., Bowers, J.B., & Agertz, O. 2019, ArXiv e-prints [arXiv:1907.08011]
- Gaia Collaboration, Babusiaux, C., van Leeuwen, F., et al. 2018a, *A&A*, 616, 10
- Gaia Collaboration, Brown, A. G. A., Vallenari, A., et al. 2018b, *A&A*, 616, 1
- Halle, A., Di Matteo, P., Haywood, M., & Combes, F. 2015, *A&A*, 578, A58
- Halle A., Di Matteo P., Haywood M., Combes F., 2018, *A&A*, 616, A86
- Jilková, L., Carraro, G., Jungwiert, B., & Minchev, I. 2012, *A&A*, 541A, 64
- Kubryk, M., Prantzos, N., & Athanassoula, E. 2013, *MNRAS*, 436, 1479
- Linden, S.T., Pryal, M., Hayes, C.R. et al. 2017, *ApJ*, 842, 49L
- Loebman, S. R., Debattista, V. P., Nidever, D. L., et al. 2016, *ApJ*, 818, L6
- Luck R. E., Lambert D. L., 2011, *AJ*, 142, 136
- Martinez-Medina, L. A., Gieles, M., Pichardo, B., & Peimbert, A., 2018, *MNRAS*, 474, 32
- Martinez-Medina, L. A., Pichardo, B., Peimbert, A., & Carigi, L. 2017, *MNRAS*, 468, 3615
- Minchev, I., Chiappini, C., & Martig, M. 2011, *A&A*, 527, 147
- Minchev, I., Chiappini, C., & Martig, M. 2013, *A&A*, 558, A9
- Minchev, I., Chiappini, C., & Martig, M. 2014, *A&A*, 781, L20
- Minchev, I., Anders, F., Recio-Blanco, A. 2018, *MNRAS*, 481, 1645M
- Minchev, I. & Famaey, B. 2010, *ApJ*, 722, 112
- Netopil, M., Paunzen, E., Heiter, U., & Soubiran, C. 2016, *A&A*, 585, A150
- Nieva, Nieva, M.-F. & Przybilla, N. 2012, *A&A*, 539, A143
- Quillen, A.C., Minchev, I., Bland-Hawthorn, J., Haywood, M., 2009, *MNRAS*, 397, 1599
- Quillen, A.C., Nolting, E., Minchev, I., De Silva, G., Chiappini, C., 2018, *MNRAS*, 475, 4450
- Quillen, A. C.; Minchev, Ivan; Bland-Hawthorn, Joss; Haywood, Misha
- Reid M. J., Menten, K. M., Brunthaler, A., et al. 2014, *ApJ*, 783, 130
- Soubiran C., Cantat-Gaudin T., Romero-Gomez M., et al. 2018, *A&A*, 619, 155
- Villanova, S., Carraro, G., Geisler, D., Monaco, L., & Assmann, P. 2018, *ApJ*, 867, 34
- Przybilla, N., Nieva, M.-F., & Butler, K. 2008, *ApJ*, 688, L103
- Roskar, R., Debattista, V. P., Stinson, G. S., Quinn, T. R., Kaufmann, T., & Wadsley, J. 2008, *ApJ*, 675, L65
- Sellwood, J. A., Binney J. J., 2002, *MNRAS*, 336, 785
- Wielen, R.; Fuchs, B.; Dettbarn, C. 1996, *A&A*, 134, 438

This paper has been typeset from a $\text{\TeX}/\text{\LaTeX}$ file prepared by the author.